

This is the accepted version of:

Rinaldi A., Mastilovic S., *The Krajcinovic approach to model size dependent fracture in quasi-brittle solids*. Mechanics of Materials, **71**: 21-33 (2014). Elsevier.

*This version of the article has been accepted for publication after peer review. The published version is available online at:*

<http://dx.doi.org/10.1016/j.mechmat.2014.01.005>

This work is licensed under the Creative Commons license

CC BY-NC-ND

URL: <https://creativecommons.org/licenses/by-nc-nd/4.0/>

1 THE KRAJGINOVIC APPROACH TO MODEL SIZE DEPENDENT FRACTURE IN  
2 QUASI-BRITTLE SOLIDS

3  
4 **Antonio RINALDI**<sup>1,2,3\*</sup> and **Sreten MASTILOVIC**<sup>4\*\*</sup>

5 <sup>1</sup> ENEA, CR Casaccia, Via Anguillarese 301, Santa Maria di Galeria, 00123, Rome, Italy

6 <sup>2</sup> International Research Center for Mathematics & Mechanics of Complex System (MEMOCS),  
7 University of L'Aquila, Via S Pasquale, 04012, Cisterna di Latina (LT), Italy

8 <sup>3</sup> ASSOINGE R&D, K. Doormanlaan 10 - 2283 AS, Rijswijk, The Netherlands

9 <sup>4</sup> Union–Nikola Tesla University, Cara Dusana 62-64, 11000 Belgrade, Serbia

10  
11 **Corresponding authors:**

12 \* [antonio.rinaldi@gmail.com](mailto:antonio.rinaldi@gmail.com)

13 \*\* [smastilovic@fgm.edu.rs](mailto:smastilovic@fgm.edu.rs)

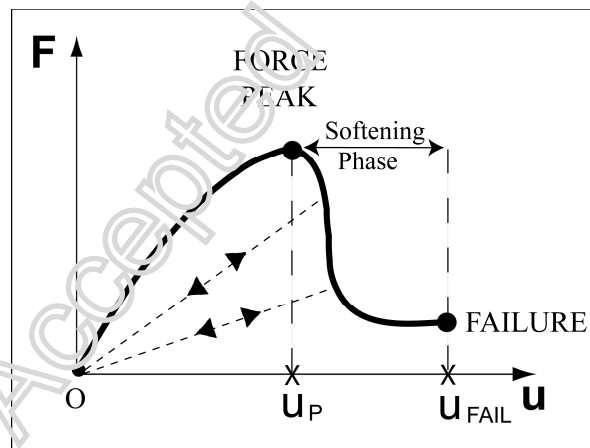
14  
15 **Key words:** failure, statistical damage mechanics, damage tolerance, size effects, fractal  
16 theory, strength scaling

17  
18 **Abstract**

19 The failure in “quasibrittle” microstructural systems, occurring with no early warning, is a  
20 debated problem of great practical importance for the structural engineering community.  
21 Available models do not fully account for typical sample-size effects observed in fracture  
22 initiation and propagation. The Krajcinovic approach (K-approach) proposed here stems from a  
23 posthumous interpretation of Krajcinovic’s original ideas and offers a new route to tackle such  
24 effects by means of an advanced fractal scheme, which consists of the sequential application of  
25 the Family-Viesek scaling laws for the number of damage events  $n(\varepsilon;L)$  in the fracture  
26 initiation and propagation regimes separately. The procedure is developed and explained in the  
27 context of an established lattice models under static tensile testing. Average simulation data for  
28 any outer-size  $L$  – here ranging from 24 to 192 - is shown to scale nicely by this method,  
29 throughout the entire damage process. The proper definition of the damage parameter  $D$  allows  
30 deploying the deduced scaling laws to deduce the actual stress vs. strain relationship applicable  
31 in engineering. The discussion extends with no prejudice to data from real experiments,  
32 provided that all necessary information is gathered and all underlying assumptions hold true.  
33 The approach shall appeal per se also to the larger scientific community of physicists and  
34 mathematicians involved in statistical mechanics and random network failure.

35 **1. INTRODUCTION: QUASI-BRITTLE FAILURE, SIZE EFFECTS AND FRACTALS**

36 Brittle, embrittled, and “quasibrittle” microstructural systems have the tendency to fail  
37 catastrophically with little or no early warning as they reach their strength, as shown in Fig.1.  
38 Besides the case of a structure containing a critical defect, such failures often develop from  
39 diffuse microcracking resulting in fracture initiation and propagation. Modeling and predicting  
40 failure of these systems is of utmost importance and has proven to be a formidable task of  
41 damage mechanics. In fact, a major complication is represented by the sample-size dependence  
42 of both the onset of strain localization and the consequent damage evolution. It is hard to predict  
43 the behavior of large structures based on laboratory tests on similarly shaped samples, unless a  
44 size-effect model (i.e. a scaling law) can be established to obtain analytical estimates. If a scaling  
45 law is available, knowledge of the statistics of a process on one scale allows inferring the  
46 statistics of the same process on any other scale. Materials systems of interest involve, for  
47 example, concrete, composites, rocks and timber, as demonstrated by a massive experimental  
48 evidence reported in literature over the past 40 years  
49



50

51 **Figure 1.** Typical tensile response of a sample made of quasi-brittle material such as concrete,  
52 failing from fracture initiation. The softening phase begins with the force peak point and ends  
53 with the structural failure. The signature feature of this behavior is the progressive loss of  
54 stiffness, as observable from the unloading paths identified solely by the secant slope in each  
55 point with no residual strain.

56

57 The modeling problem has been under investigation for centuries and many researchers have  
 58 attempted a number of different strategies. Some modern approaches to fracture and damage  
 59 have originated from fractal theory and lattice models. For instance, Mishnaevsky Jr (1996)  
 60 monitored the surface roughness of crack and the specific surface energy needed to form a  
 61 crack by the mechanism of microcrack coalescence and concluded that the fractal dimension of  
 62 crack may be monitored during the crack formation process to compute the time-to-fracture in  
 63 heterogeneous solids. Another group (Cherepanov et al. 1995, Balankin et al. 1996) suggested  
 64 that the usual LEFM expressions for stress concentration at the crack tip could be replaced by a  
 65 fractal version based on a roughness-related power law exponent  $\alpha$  and a fractal stress intensity  
 66 factor  $K_f$  as

$$67 \quad \sigma_{ij} \propto K_f \frac{r^{-\alpha}}{l_0} \quad (1)$$

68 when crack length  $l$  falls between a lower cut-off  $l_0$  and a self-affine correlation length  $\zeta$ ,  
 69  $l_0 < l < \zeta$ . Similar continuum-based approaches have followed (Borodich 1997) with some  
 70 noteworthy contributions that include for example the “Quantized Fracture Mechanics for fractal  
 71 cracks” (Pugno and Ruoff 2004, Wnuk and Yavari 2008) or the fractional continuum framework  
 72 of fracture and damage discussed by Tarasov (2013) and Ostoja-Starzewski et al. (2007,2013).  
 73 As far as damage initiation in quasi-brittle materials, Carpinteri and coworkers (e.g., 1994, 2012)  
 74 devoted substantial effort to size-effects inherent to fracture in concrete and proposed what they  
 75 called multi-fractal scaling laws for the strength  $\sigma_{PEAK}$ , which we can rewrite here as:

$$76 \quad \sigma_{PEAK} \propto \sigma_{PEAK}^* L^{-\beta} \quad (2)$$

77  
 78  
 79 where  $\sigma_{PEAK}^*$  is a scale invariant material parameter,  $\beta$  is the fractal exponent ranging from 0 to  
 80  $\frac{1}{2}$ , for the low and high material heterogeneity limits respectively, and  $L$  is the sole significant  
 81 geometrical parameter, provided that only self-similar samples are compared. When applied to  
 82 experimental data, the authors stated that Eq.(2) provides an empirical method to obtain  
 83 reasonable values for the fractal dimension damage domain, barring the existence of excessive  
 84 scatter in the experimental data. They also documented a good agreement with the microcracking

85 process as measured from the acoustic emission (AE) experiments, recovering the power-law and  
86 intermittency of avalanches of AE events, as well as the fractal distributions of event locations.

87 Nonetheless, the multi-scale approach faced also some criticism from exponents of civil  
88 engineering community, primarily by Bazant and co-workers. Following an alternative rationale,  
89 Bazant (1997a, 1997b) first developed an asymptotic argument and proposed a different model  
90 for the fracture initiation problem

91

$$92 \quad \sigma_{PEAK} = \sigma_{PEAK}^* \left( 1 + \frac{A}{B+L} \right)^{-1/\beta} \quad (3)$$

93 where A and B are fitting constants. In subsequent papers (2004, 2005), Bazant and co-workers  
94 reported a thorough overview of size effects and scaling laws for many different structural  
95 systems based on their approach, pointing out the affinity with Weibull statistics and strongly  
96 advocating weaknesses of fractal-based models such as (2).

97 However, a third-party work by Karihaloo and co-workers (Ince et al. 2003) found  
98 merits in both approaches when comparing approach (2) vs. (3), one outperforming the other in  
99 different size ranges, which ushers in the possibility for such dispute to live on unsettled. At the  
100 same time there is the general view in the engineering community that modeling size-effects  
101 remains a fertile and urgent research ground for the sake of establishment of reliable models and  
102 improvements of current design codes in structural engineering.

103 In this paper we present a different scaling procedure that we will call “Krajcinovic  
104 approach” (K-approach hereafter) as this stems from our posthumous revision of seminal ideas  
105 and prior work headed by Dusan Krajcinovic. The original papers by Krajcinovic and Rinaldi  
106 (2005a, 2005b) and Rinaldi et al. (2006, 2007) laid the foundation of the work presented here  
107 and fostered the usage of fractal theory in connection with lattice model, in a manner very  
108 different from Carpinteri’s. Rather than concentrating on the fracture strength, Krajcinovic’s  
109 initial exploration focused on establishing the connection between a random heterogeneous  
110 microstructured material and the damage parameter  $D$  in the constitutive relation throughout  
111 the damage process, from the early stage microcracking to the final crack propagation.  
112 Noteworthy,  $D$  enters the constitutive relations of a material but it is not an intrinsic property,  
113 being associated to given boundary conditions and a given loading history. For example, unlike  
114 comminution damage in fragmentation problem where the complete loss of stiffness is not

115 achieved at failure (e.g. Mastilovic and Krajcinovic, 1999a, 1999b), the damage parameter for  
116 the tensile test is strictly related to loss of stiffness such as  $D=\Delta E/E_0$  (Rinaldi, 2009).

117 Since the damage evolution is a stochastic process that depends on applied load and  
118 microstructural disorder of a given sample (i.e. random texture and imperfections),  $D$  is a  
119 random variable and the problem is better stated in terms of representative average  $\langle D \rangle$   
120 (Rinaldi, 2009). More precisely, the macroscale stress-strain response of a damaged  
121 heterogeneous quasi-brittle material subject to strain-controlled quasi-static uniaxial test is  
122 customarily expressed by the Kachanov's relation<sup>1</sup>

$$123 \quad \langle \sigma(\boldsymbol{\varepsilon}) \rangle = E_0(1 - \langle D(\boldsymbol{\varepsilon}_0; L) \rangle) \boldsymbol{\varepsilon} \quad (4)$$

124 where  $\langle \sigma \rangle$  is the average stress response associated to the imposed strain level  $\boldsymbol{\varepsilon}$ ,  $E_0$  is the  
125 initial Young's modulus, and the expected value of the damage parameter  $\langle D(\boldsymbol{\varepsilon}_0; L) \rangle$  depends  
126 on the loading history  $\boldsymbol{\varepsilon}_0$  (i.e., in this case, the maximum strain applied) and on the sample size  
127  $L$ . When structural healing is prevented, the damage effect is detected at the macroscale by the  
128 (permanent) loss of secant stiffness  $\langle E(\boldsymbol{\varepsilon}) \rangle = E_0(1 - \langle D(\boldsymbol{\varepsilon}_0; L) \rangle)$  associated with the microcracking  
129 process, ranging from  $\langle E(\boldsymbol{\varepsilon}) \rangle = E_0$  for  $\langle D \rangle = 0$  (i.e. no damage) to  $\langle E(\boldsymbol{\varepsilon}) \rangle = 0$  for  $\langle D \rangle = 1$  at failure.  
130 Krajcinovic's original intention was to scale the average response of a brittle material in Eq. (4)  
131 by identifying a suitable scaling law for  $\langle D \rangle$

$$132 \quad \langle D(\boldsymbol{\varepsilon}_0; L) \rangle = f(L) \quad (5)$$

133 which was sought by means of a fractal-based procedure. However, despite some recognition  
134 (e.g. Carpinteri et al., 2012), his ideas were substantially overlooked by the scientific  
135 community at large, partly because the fundamental concepts were probably reported in  
136 fragmentary and yet incomplete way. The primary objective of this paper is to fill this gap and  
137 describe a new scaling procedure in a unitary and finalized form, linking it to prior attempts  
138 and explaining in practical terms its usage to practitioners. The method will be illustrated on  
139 numerical data from discrete lattice models of different size  $L$ . Succinct commentaries of some

---

<sup>1</sup> Note that a similar (internal variable) constitutive model was applied lately in the context of friction wear by D'Annibale and Luongo.

140 percolation and finite-size scaling ideas that immediately relate to the lattice models and to the  
141 K-approach are presented first.

## 142 **2. HISTORICAL PERSPECTIVE OF STATICAL METHODS FOR LATTICES**

143 Although fracture models are of primary importance to the structural engineering community, the  
144 subject has always appealed significantly to physicists and mathematicians, especially among the  
145 statistical mechanics community, which bred a substantial body of results and ideas that are the  
146 cornerstone of the methods cited above including ours. Noteworthy, these results flourished over  
147 the past 30 years in conjunction with discrete lattice models that provided the possibility to  
148 simulate realistically the microstructural disorder of materials and reproduce structural size-  
149 effects in a tractable manner. Let us briefly recall the main statistical methods applied to failure  
150 of quasi-brittle lattice (ref. Krajcinovic 1996).

### 151 **2.1 Percolation theory of damage in discrete models**

152 Percolation theory is one of the earliest and simplest approaches to investigate phase transitions  
153 in statistical physics (e.g., Stauffer and Aharony, 1994) and has been applied with some success  
154 to geometrical and transport properties of mechanical lattices, along with size effects. A damaged  
155 lattice can be indeed regarded as a random graph of connected clusters and, as such, it can be  
156 studied by means of percolation theory. In that view failure is treated as a phase transition that  
157 occurs at percolation condition, that is when the correlation length  $\xi$ , associated to the  
158 connected/interacting clusters of microcracks, spans the entire finite-size lattice  $L$  (or diverges  
159 for an infinite lattice as  $L \rightarrow \infty$ ). The percolation threshold  $p_c$  is defined as the occupation  
160 probability  $p$  at which an infinite cluster appears in the lattice according to a power-law fractal  
161 exponent  $\nu$

$$162 \quad \xi \propto |p_c - p|^{-\nu} \quad (6)$$

163 For a mechanical network,  $p$  roughly corresponds to the density of unbroken springs and  $p_c$  is  
164 critical point associated to failure. The threshold  $p_c$  is defined with respect to an infinite lattice  
165 and approached asymptotically in the limit of  $L \rightarrow \infty$ . The application of the results to finite-  
166 size systems happens by renormalization group approaches, such as coarse graining techniques  
167 (e.g. Christensen, 2002).

168 Similar scaling laws were sought for many other and diverse parameters (e.g., connectivity,  
169 number of microcracks, etc.) and network transport properties (e.g., conductivity, stiffness,  
170 etc.) related to the “failure transition” and thereby exhibiting a singularity. As an example, Sen  
171 et al. (1985) studied the percolation model for the central-force elastic lattice, finding that bulk  
172 modulus ( $K$ ) and shear modulus ( $G$ ) scaled as

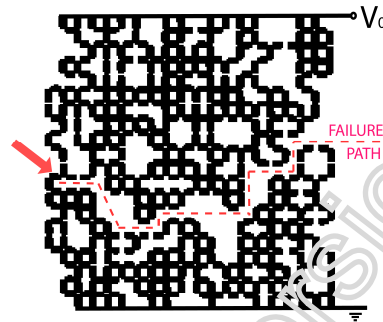
$$173 \quad K, G \propto (p - p_c)^\beta \quad (7)$$

174 with the following numerical estimates  $p_c = 0.58$ ,  $\beta = 2.4 \pm 0.4$  for 2D triangular lattices and  
175  $p_c = 0.42$ ,  $\beta = 4.4 \pm 0.6$  for 3D face centered cubic (FCC) lattices. The same group proposed an  
176 effective medium theory of spring-network models, mapping the percolation property of the  
177 central-force lattice to a continuum scale, also exploring importance of the coordination number  
178 of lattice sites on the scaling (Feng et al. 1985). Many authors (Chelidze 1982, Roux and Guyon  
179 1985, Ostoja-Starzewski 1989, etc.) have reported similar results but, despite the apparent  
180 simplicity, the application of percolation ideas to damage has proved to be not straight forward.  
181 Krajcinovic (1996) offered a detailed essay on this subject, stressing the importance of  
182 percolation theory in damage mechanics and its limitations. Percolation theory ought to be  
183 regarded as complementary to mean-field theories of continuum mechanics (e.g. dilute  
184 concentration models of damage), granting a way to approach size-scaling issues by means of  
185 relations that are universal and supposedly independent of microstructural details. Hansen and  
186 Roux (1989), amongst others, investigated the universality problem for central-force lattices.  
187 However, one main problem is the estimation of fractal exponents associated to asymptotic  
188 behaviors, which require large computations. In time, successive reports have modified earlier  
189 accounts and larger simulations have indicated that fracture damage may not comply with basic  
190 (uncorrelated) percolation process (Nukala et al. 2006). Another drawback inherent to some  
191 percolation studies resides in the preservation of isotropy during the percolation process that  
192 proceeds by random either suppression/strengthening of links (e.g. Garcia-Molina et al. 1988),  
193 which makes them ill posed to study damage induced anisotropy that immediately arise in  
194 quasi-brittle (vectorial) systems (Rinaldi 2009). A critical review by Guyon et al. (1990)  
195 represents a relevant and insightful reading on the subject.



196 **2.2 Fractal scaling laws of damage in discrete models**

197 Besides percolation models, lattice models represent a fertile playground for the application of  
198 many other methods of statistical physics. The fuse lattice by De Arcangelis et al. (1985)  
199 illustrated in Fig. 2 is one of the first attempts to depart from percolation ideas and introduce  
200 damage by a more realist mechanism of fuse burn-out caused by quenched or annealed disorder  
201 as opposed to random link suppression (Krajcinovic 1996).



202

203 **Fig. 2.** Example of fuse lattice at the onset of failure, where the suppression of the last fuse  
204 pointed by the arrow leads to failure (zero conductance) (redrawn from De Arcangelis et al.  
205 1985).

206

207 These fuse models drew immediately a great attention (e.g. Duxbury et al 1986, Alava et al.  
208 2006) as simple scalar models of failure in heterogeneous solids, but were immediately sided  
209 by actual “vectorial” mechanical models such as beam and central-force lattices. The latter are  
210 indeed significantly more complex and realistic, especially as far as the damage-induced elastic  
211 anisotropy and failure patterns are concerned.

212

213 The research scope also expanded to consider not just the scaling of one critical point  
214 corresponding to the failure threshold, like in percolation, but the entire response of the system  
215 during the damage process, particularly after strain localization. The objective was to establish  
216 fractal-based transformations that succeed in reconciling the mechanical response of samples  
217 of any size by mapping their mechanical response into one scale invariant curve, thus yielding  
a scaling law for the given damage process.

218 **2.2.1 Family-Vicsek scaling**

219 For our discussion, one specific method called the Family-Vicsek scaling (Family and Vicsek  
 220 1991, Barabasi and Stanley 1995) stands prominently above others. It was first used for growth  
 221 of advancing solidification fronts at the liquid-solid interface. Let us consider the generic  
 222 function  $y(x, L)$  as dependent on a variable  $x$  defined over a network domain but also on the  
 223 size  $L$  of the network itself, as depicted in Fig. 3a. The knee-shape typically marks a phase  
 224 transition at the critical point location  $(x^*, y^*)$ .

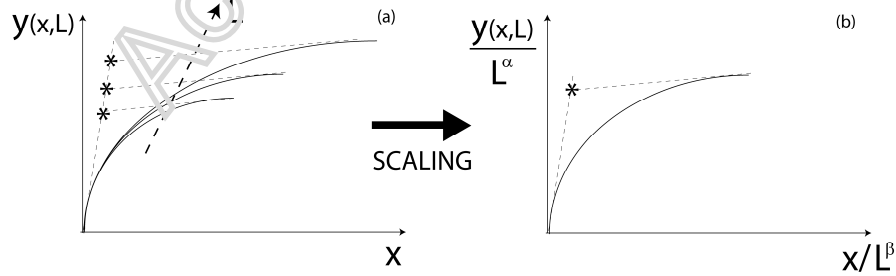
225 If the Family-Vicsek scaling holds, then the data  $y(x, L)$  shall map onto one universal scale-  
 226 invariant curve such that  $f(x/L^\beta, y/L^\alpha) = y/L^\alpha$  for any  $L$ , as indicated in Fig. 3b, according to the  
 227 following scaling relation

228 
$$y(x, L) = L^\alpha f\left(\frac{x}{L^\beta}\right) \tag{8}$$

229 Three conditions must be met for this scaling procedure to be feasible:

- 230 1. at the transition the  $y$  value must be a fractal such that  $y(x^*, L) \propto L^\alpha$ ,  
 231 2. the location of the transition must be a fractal such that  $x^* \propto L^\beta$ ,  
 232 3. before the transition the data must follow a power law  $y(x, L) \propto x^\gamma$ .

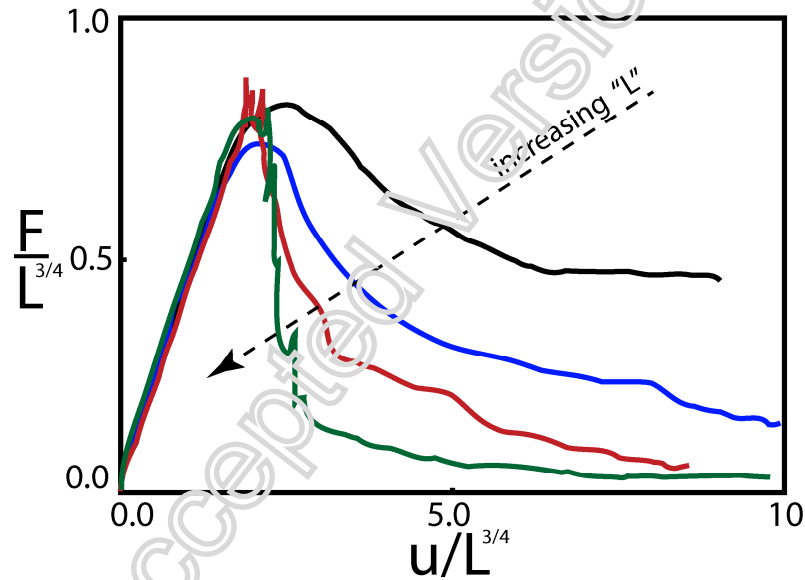
233 Consequently only two out of the three exponents  $\{\alpha, \beta, \gamma\}$  are independent due to the  
 234 constraint  $\gamma = \alpha / \beta$ .



235

236 **Fig.3.** Illustration of the scaling procedure applicable to some non-linear systems that  
 237 experience a transition governed by a universal law. The response  $y$  depends on the controlled  
 238 variable  $x$  but also on the system size  $L$ , which controls the occurrence of the transition. A  
 239 scaling law exists if  $y(x,L)$  maps into a scale invariant curve upon normalizing  $y$  and  $x$  by  $L^\alpha$   
 240 and  $L^\beta$  respectively.

241 This empirical scaling procedure, borrowed from phase transitions and clusters theory, has  
 242 proved useful to investigate microcracks cooperation and damage localization in multisite  
 243 cracking and fracture processes, where lattice models had already revealed the existence of  
 244 several fractals quantities. Hermann, Hansen and Roux sought to apply the scaling to data from  
 245 numerical experiments on central-force lattice (Hansen et al. 1989) and beam lattice (Hermann  
 246 et al. 1989), finding satisfactory results only over certain portions of the damage process. Fig. 4  
 247 displays raw force-displacement data  $F(u)$  for the beam lattice vs. scaled data  $F = L^\alpha f(uL^{-\beta})$   
 248 with scaling exponents  $\alpha = \beta = 0.75$ . They also sought a scaling relation for other quantities,  
 249 such as the number of broken links  $n = L^\gamma \Psi(uL^{-\beta})$ . The results of the scaling displayed in Fig. 4  
 250 exemplifies that the scaling could be used only up to the force peak.



251  
 252 **Fig. 4.** Results of Family-Vicsek scaling (data from Hermann et al. 1989).

### 253 3. The K-approach

254 The Family-Vicsek scaling is also the cornerstone of the approach featured here, although  
 255 utilized in a much different manner, along the footsteps of Krajcinovic. As opposed to Fig.4  
 256 (and to most other scaling in literature), our strategy does not target the force vs. displacement  
 257 data directly, but it pursues the nested application of the Family-Vicsek scaling (8) on the  
 258 curves  $n-\varepsilon$  (i.e., number of microcracks vs. strain), which resemble the situation sketched in  
 259 Fig.3. Note that it is not possible to scale  $n-\varepsilon$  with a single application of Eq.(8) because the

260 damage process encompass two stages, each governed by different fractal quantities. Let us  
 261 first state the principle of our scaling, and then explain the practical application on an example.

262

263 **Statement #1.** The objective of the K-approach is twofold: (i) the formulation of scaling laws  
 264 for the  $n(\varepsilon; L)$ , mapping these data into a scale-invariant function valid for any  $L$ , and (ii) the  
 265 linking of such scaling function to the damage parameter  $D$ .

266 **Statement #2.** The practical procedure consists of applying the Family-Vicsek twice in  
 267 cascade, according to a two-steps scheme entailing the sequential application of (8) separately  
 268 to the microcracks prior and after the stress peak, in recognition of the nature of the fracture  
 269 initiation problem consisting of two distinct phases (ref. Fig.6 later). The two steps are:

270 **Step #1:** Application of Eq.(8) to the number of microcracks and, by setting  $\alpha=d+\beta$  ( $d$   
 271 is the applicable Euclidean dimension), the identification of the sole independent fractal  
 272 exponent  $\beta$  that makes the scaled data " $n(\varepsilon, L) / L^{d+\beta}$  vs.  $\varepsilon/L^\beta$ " overlap for any  $L$  up to the peak  
 273 strain  $\varepsilon_p$ , thus yielding the scale-invariant function  $g(\varepsilon/L^\beta)$

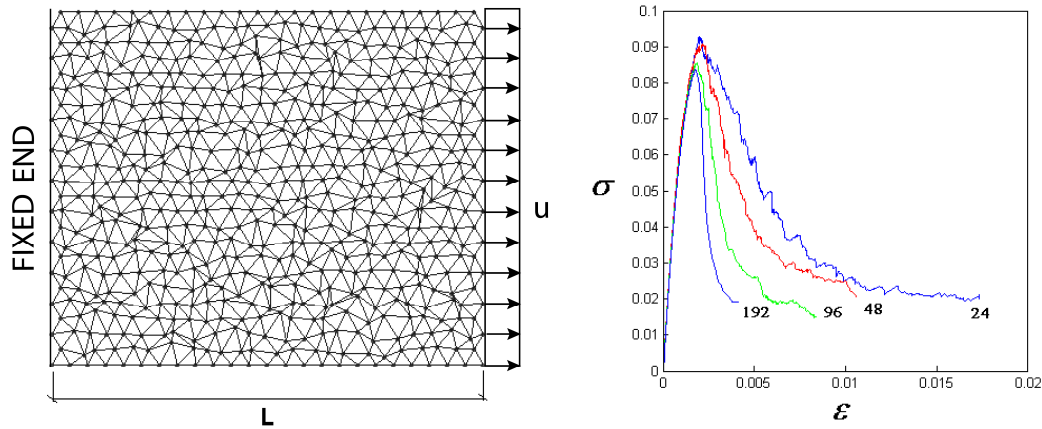
274 
$$n(\varepsilon; L) = L^{d+\beta} g\left(\frac{\varepsilon}{L^\beta}\right) \quad (9)$$

275 **Step #2:** Nested application of Eq.(8) to the post-peak increment of microcracks  $\Delta n$  and  
 276 identification of the exponent  $\beta'$  that delivers a scale invariant function  $g'(\Delta\varepsilon/L^{\beta+\beta'})$ , making the  
 277 remaining data of the softening phase overlap for any  $L$  up to failure.

278 
$$\Delta n(\varepsilon; L) = L^{d+\beta+\beta'} g'\left(\frac{\Delta\varepsilon}{L^{\beta+\beta'}}\right) \quad (10)$$

279 **3.1 Example: application to lattice data**

280 The procedure is illustrated here with respect to the same simulation data used originally by  
 281 Krajcinovic and Rinaldi (2005a, 2005b) for the random lattice of size  $L \times L$  depicted in Fig.5,  
 282 the details of which are recalled in the Appendix. Therein, the average stress responses from  
 283 the tensile tests for each  $L$  represent the primary output from simulations, clearly  
 284 demonstrating the existence of a strengthening effect with the shrinking  $L$ , like in real systems.

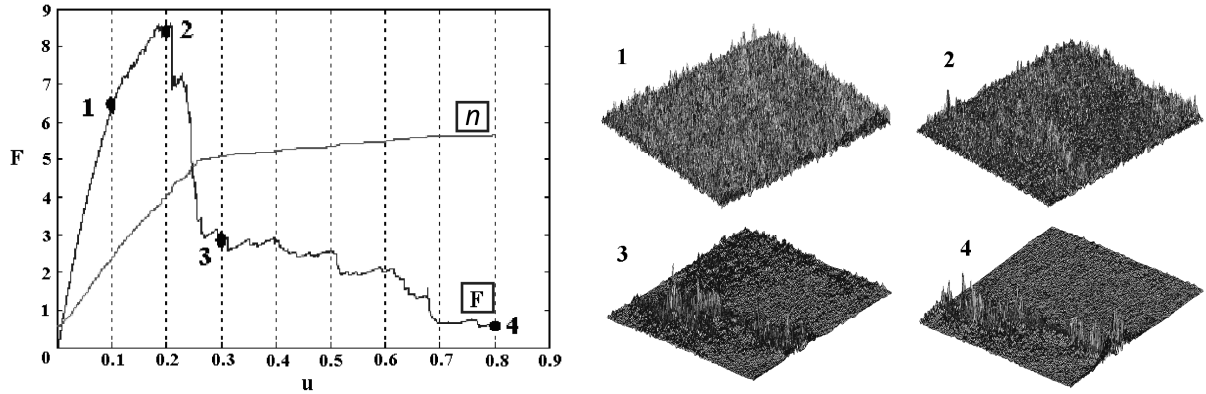


285

286 **Fig. 5.** Irregular triangular lattice of square shape ( $L \times L$ ) subjected to uniaxial tensile load in a  
 287 displacement controlled mode. Average stress vs. strain response for  $L = \{24, 48, 96, 192\}$   
 288 computed over 10 replicates per size.

289

290 However, the K-scaling requires “tracking” the function of broken links (i.e. the microcracks)  
 291  $n(\epsilon; L)$ , which is the object of the scaling. The function  $n(\epsilon; L)$  is often recognized as the  
 292 primary source of information about the damage process and is indeed closely related to the  
 293 damage parameter  $D$ . In 1-D models, the function  $n(\epsilon)$  is actually all that is needed to compute  
 294  $D$ , usually through a closed-form solution (Rinaldi 2011). In higher dimensional problems such  
 295 as this 2-D lattice lattice, this connection still exists but is more complex, as demonstrated  
 296 earlier (Rinaldi, 2009). The sample data plotted in Fig.6 allows grasping such a connection  
 297 between the force response and the microcracks evolution. The micro-stress fields are  
 298 compared (in absolute value) at four states of the damage process. While the micro-stress  
 299 distribution "1" is statistically "invariant" for all replicates with same size  $L$  and corresponds to  
 300 random damage nucleation, the distributions "2, 3, and 4" all depend on the disorder of the  
 301 microstructure and reveal damage localization and propagation. The knee in the  $n-u$  curve,  
 302 overlaid (out of scale) onto the  $F-u$  data, is reminiscent of the scenario in Fig.3 and marks the  
 303 occurrence of the transition between this two regimes, from homogeneity to heterogeneity  
 304 (equivalently from nucleation to propagation of damage or from hardening to softening). As  
 305 discussed elsewhere (Rinaldi, 2007, 2009), damage nucleation is a “diffuse” process with  
 306 higher rupturing rate whereas damage propagation is a process highly correlated in space and  
 307 with a (apparently) lower microcracking rate.

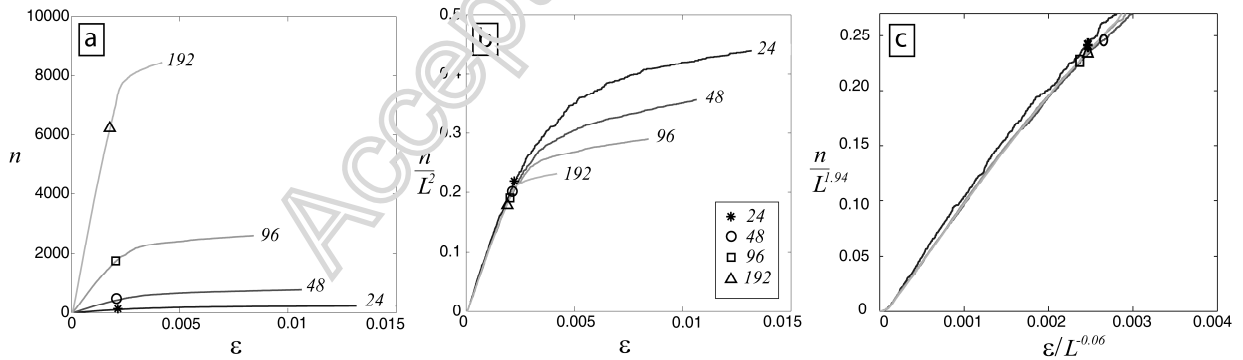


308

309 **Fig.6.** Micro-stress distribution at 4 points of the damage process. Stress (strain) localization is  
 310 observed at “2” (peak point) from the loss of statistical homogeneity and formation of energy  
 311 (stress) clusters (i.e. hot-spots).

312 In our case, the average  $n-\varepsilon$  curves associated to the stress curves in Fig.5 are plotted per each  
 313  $L$  in Fig.7a. Remarkably, the proposed scaling procedure can be illustrated on such lattice data  
 314 with no loss of generality since it applies seamlessly to real systems, being the needed  $\sigma-\varepsilon$  and  
 315  $n-\varepsilon$  data in Figs. 5 and 7 obtainable also experimentally, e.g. through AE techniques (e.g.  
 316 Carpinteri et al. 2012).

317



318

319 **Fig. 7.** Plots of (a)  $n-\varepsilon$ , (b)  $\rho-\varepsilon$ , (c)  $g-\varepsilon$ . (b) Normalizing  $n$  by  $L^2$  yields a microcracks density  
 320  $\rho$  and produces a first substantial data overlap regardless of  $L$ ; yet, the marked peak points  
 321 depend on  $L$ . (c) Scaling data from (b) to (c) causes data collapse up to the peak and renders the  
 322 complete Family-Vicsek in Eq.(9) for  $n(\varepsilon;L)$ .

323 **3.1.1. Step#1: pre-peak region**

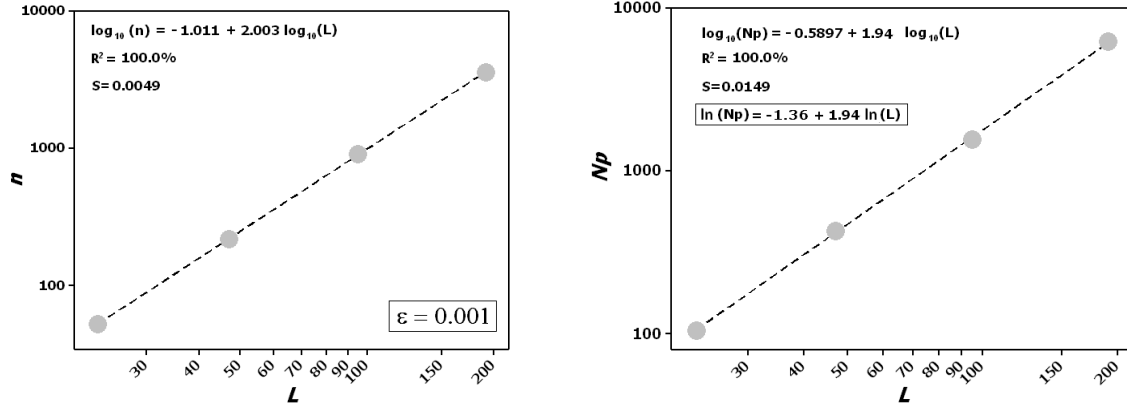
324 With regard to the Step#1 of the procedure, the best results shown in Fig.7c are obtained for  
325 the exponent  $\beta=-0.06$  in the scaling Eq.(9), which specializes as

326 
$$n(\boldsymbol{\varepsilon}, L) = L^{1.94} g\left(\frac{\boldsymbol{\varepsilon}}{L^{-0.06}}\right) \quad (11)$$

327 A substantial overlap is achieved from (11) among all transformed datasets, with near-  
328 clustering of all peak points. Accuracy of this deduction is always limited in reality by the  
329 finiteness of the simulation/experimental sample, which is used to infer an asymptotic  
330 property, i.e. the scale invariant transformation  $g(\boldsymbol{\varepsilon}/L^\beta)$ .

331 Apart from practical usage, a few observations help gaining a better insight of Eq.(9)  
332 and about the rationale underlying step#1. Let us note first that the intermediate normalization  
333 of  $n$  by  $L^{d-2}$  in Fig.7b renders an “average microcracks density”  $\rho = n/L^2$  and produces a  
334 substantial data collapse and causes all transformed curves to exhibit equal slope. This  
335 intermediate result had been observed phenomenologically (e.g. Hansen et al., 1989) and has  
336 been demonstrated to be necessary on a theoretical ground by Rinaldi (2007). However, this  
337 does not suffice to deliver a scale invariant, because the peak strains are still different. Then, a  
338 subsequent Family-Vicsek transformation bring us from Fig.7b to Fig.7c by using the  
339 constraint  $\alpha=\beta=-0.06$  in Eq.(8) to map the peak points into one while preserving the slope  
340 agreement. Such a logical construction is evidently reflected in Eq.(9).

341 In agreement with the fundamental hypotheses of the Family-Vicsek scaling enlisted in  
342 Section 2.2.1, the successful scaling in Fig.7c implies that that the number of microcracks at  
343 the peak  $N_p$  and peak strain are both fractal quantities that scale as  $N_p \propto L^{d-\beta}$  and  $\boldsymbol{\varepsilon}_p \propto L^\beta$   
344 respectively. In support of this view, in Fig.8 we can check that the microcracks scale as  
345  $n(\boldsymbol{\varepsilon}; L) \propto L^2$  before the peak and as  $n(\boldsymbol{\varepsilon}_p; L) = N_p \propto L^{1.94}$  at the peak, in agreement with  
346 Fig.7c.



347

348 **Fig.8.** Comparison of fractal behavior of  $n(\varepsilon;L)$  at  $\varepsilon = 0.001$  vs. peak strain ( $N_p$ ), demonstrated  
 349 by the linearity of  $\log(n)$  vs.  $\log(L)$ . In the former case the exponent is  $\sim 2$  and lowers to  $\sim 1.94$   
 350 at the peak, matching Fig.7c. For convenience-sake, the power law of  $N_p$  is expressed also in  
 351 base e such that  $N_p = e^{-1.36} L^{1.94}$ .

352

353 Next, we need to determine the damage parameter  $D$  valid up the strain peak for the system  
 354 under consideration. Based on the results from Krajcinovic and Rinaldi (2005a), our lattice is  
 355 known to behave in a manner identical to the corresponding “fiber bundle model” (see  
 356 Appendix) and we can adopt the following definition,

357 
$$D(\varepsilon;L) = \frac{n(\varepsilon;L)}{2N_p} \quad (12)$$

358 To conclude our task, by virtue of Eq.(11) and because  $N_p = e^{-1.36} L^{1.94}$  from Fig.8, we can rewrite  
 359 it in scale-invariant form as

360 
$$D(\varepsilon) = \frac{g(\varepsilon/L^{-0.06})}{2e^{-1.36}} \quad (13)$$

361 An analytical form can be obtained by replacing  $g$  with an approximating function fitted to the  
 362 data in Fig.7c in different ways, e.g. via regression methods. In this case, we can for example  
 363 assume the linearity  $n/L^{1.94} \propto \varepsilon/L^{-0.06}$  throughout the range and perform a first order Taylor  
 364 expansion around  $\varepsilon=0$  such that “ $n/L^{1.94} = \partial(n/L^{1.94})/\partial(\varepsilon/L^{-0.06})|_{\varepsilon=0} \cdot \varepsilon/L^{-0.06}$ ”, which leads to

365 
$$g(\varepsilon/L^{-0.06}) = \partial\rho/\partial\varepsilon|_{\varepsilon=0} \frac{\varepsilon}{L^{-0.06}} \quad (14)$$



366 with  $\partial\rho/\partial\varepsilon|_{\varepsilon=0}$  being evaluated numerically as the initial slope either in Fig.7b or Fig.7c. The  
 367 damage parameter is estimated as

$$368 \quad D(\varepsilon) = \frac{\partial\rho/\partial\varepsilon|_{\varepsilon=0} \cdot \varepsilon}{2e^{-1.36} L^{-0.06}} \quad (15)$$

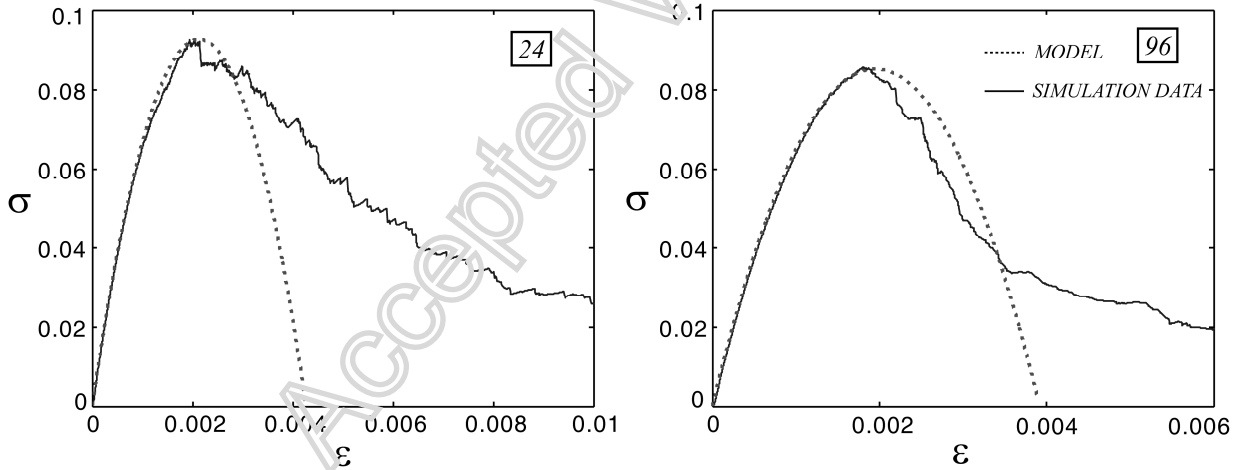
369 For this specific example the value of the damage parameter at the peak is invariably  $D_p=0.5$ .  
 370 The corresponding peak strain, marking the range of validity of Eq.(13), is

$$371 \quad \varepsilon_p = \frac{e^{-1.36}}{\partial\rho/\partial\varepsilon|_{\varepsilon=0}} L^{-0.06} \quad (16)$$

372 and Eq.(12) can be back-computed in terms of strain as

$$373 \quad D(\varepsilon;L) = \frac{\varepsilon}{2\varepsilon_p} \quad (17)$$

374 The results of the Eq.(18) vs. simulation data provide the validation of the formulated model.



375  
 376 **Fig.9.** Mean response from simulation data (solid line) plotted vs. constitutive model Eq. (4)  
 377 (dotted line) from the damage definition Eq.(12) for  $L=24,96$ . The model appears accurate up  
 378 to the peak and, expectedly, deviates from simulations afterwards.

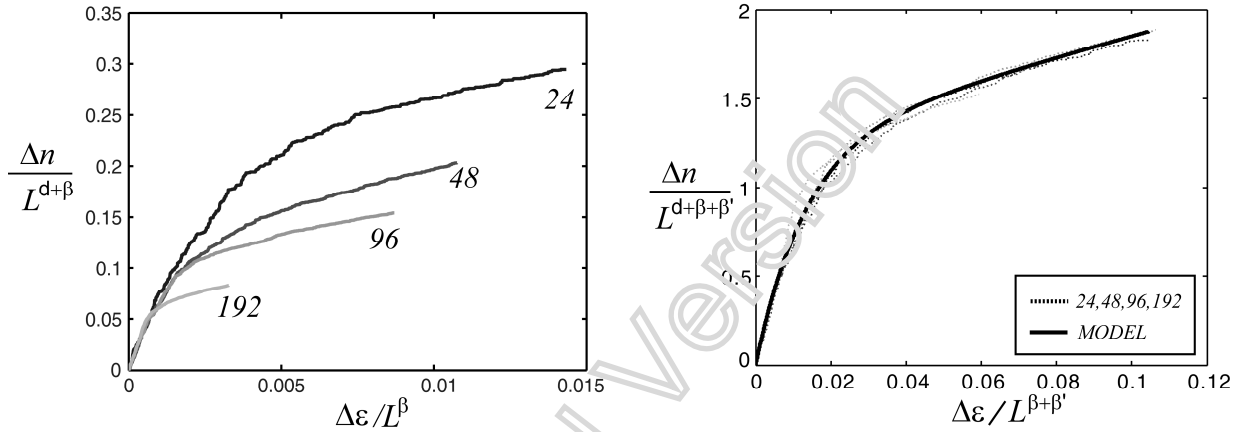
379

380 **3.1.2. Step#2: post-peak region**

381 The step#2 of the K-approach proceeds in an analogous manner but focuses exclusively on the  
 382 post-peak data  $\Delta n$  vs.  $\Delta \varepsilon$ , with  $\Delta n = n - n_p$  and  $\Delta \varepsilon = \varepsilon - \varepsilon_p$ . The best results are displayed in  
 383 Fig.10 and are obtained for  $\beta' = -0.54$ , such that Eq.(10) can be rewritten as

384 
$$\Delta n(\varepsilon, L) = L^{1.40} g' \left( \frac{\Delta \varepsilon}{L^{-0.60}} \right) \quad (18)$$

385



386 **Fig.10.** (a) Post-peak data after the transformation Eq.(9) and (b) results from step#2 of the K-  
 387 approach bringing all datasets fall into one scale invariant function  $g'(\Delta \varepsilon / L^{\beta+\beta'})$  for  $\beta' = -0.54$  in  
 388 Eq.(10).  
 389

390

391 The scaling function  $g'(\Delta \varepsilon / L^{\beta+\beta'})$  is well approximated by the following analytical function  
 392 (Fig. 10b - solid line)

393 
$$g'(\Delta \varepsilon / L^{\beta+\beta'}) = a_1 \frac{\Delta \varepsilon}{L^{\beta+\beta'}} + b_1 \left[ 1 - \exp \left( -c_1 \frac{\Delta \varepsilon}{L^{\beta+\beta'}} \right) \right] \quad (19)$$

394 where the fitting parameters are ( $a_1 = 6$ ,  $b_1 = 1.25$ ,  $c_1 = 75.2$ ) for our data. The latter ones are not  
 395 independent and the two following conditions

396

397 
$$a_1 + b_1 c_1 = \left. \frac{\partial n}{\partial \varepsilon} \right|_{\varepsilon_p} \quad (20)$$

398 
$$a_1 = \left. \frac{\partial n}{\partial \varepsilon} \right|_{\infty} \quad (21)$$

399

400 can be imposed onto the scaled  $\partial n / \partial \bar{\varepsilon}$  in order to:

401 1. to maintain a  $C^1$  continuity with data pre-peak data from Eq.(14) and

402 2. to insure the correct asymptotic failure rate.

403 The terms on the right-hand side in Eqs.(20,21) are measurable from Fig.10b. Thus, since  $a_1$  is  
404 imposed, only one free parameter is left and the pair  $\{b_1, c_1\}$  is selected to optimize the data fit  
405 of Eq.(19). Combining Eqs.(18) and (19) yields the desired scaling law for the microcracks  $\Delta n$   
406 in the propagation regime

$$407 \quad \Delta n(\varepsilon, L) = L^d a_1 \Delta \varepsilon + L^{d+\beta+\beta'} b_1 \left[ 1 - \exp\left(-c_1 \frac{\Delta \varepsilon}{L^{\beta+\beta'}}\right) \right] \quad (22)$$

408 Next, the determination of the damage parameter for the softening phase requires a  
409 model, similarly to Eq.(12) for step#1. Because damage is additive, the softening damage  
410 simply sums up to the amount previously cumulated up to the peak strain with the new  
411 increment

$$412 \quad D(\varepsilon; L) = D_p + \Delta D(\varepsilon, L) \quad (23)$$

413

414 where  $\Delta D = D - D_p$  and  $D_p = 0.5$  from Eq.(17). To this purpose, we can recall and use the model  
415 developed by Rinaldi et al (2006) by seeking to identify the damage increment  $\Delta D$  from  
416 normalizing  $\Delta n$  by an appropriate factor  $X(L)$

$$417 \quad \Delta D(\varepsilon, L) = \frac{\Delta n}{X(L)} \quad (24)$$

418 The determination of  $X(L)$  is pursued through statistical methods to reach a "data driven"  
419 decision. According to standard ordinary least square (OLS) regression methods, the stress  
420 estimate  $\hat{\sigma}_i$  in correspondence to  $\varepsilon_i$  and  $\Delta n_i$  at the generic  $i$ -th point of the stress response Eq.(4)

421 was expressed as

$$422 \quad \hat{\sigma}_i(\varepsilon_i, \Delta n_i, X) = E_0 [0.5 - \Delta n_i / X] \varepsilon_i, \quad (25)$$

423 where  $X$  is the target parameter to be estimated. Since this model is linear in  $1/X$ , the OLS  
424 method can be used to compute a minimum unbiased estimator  $\hat{X}$  the minimization of the error

425 function  $Err(1/\hat{X}) = \sum_{i=1}^Q (\bar{\sigma}_i - \hat{\sigma}_i)^2$  over  $Q$  simulation points by setting  $\partial Err / \partial \hat{X} = 0$  leads to

426

$$\hat{X}(L) = \frac{\sum_{i=1}^Q \bar{K}_0 \bar{\varepsilon}_i^2 \Delta n_i^2}{\sum_{i=1}^Q \left( \left[ (1 - D_p) \bar{K}_0 \bar{\varepsilon}_i - \bar{\sigma}_i \right] \Delta n_i \bar{\varepsilon}_i \right)} \quad (26)$$

427

428 The estimates from Eq.(26) are displayed in Fig.11 with circles (note that extra data for  
429  $L=\{72,120\}$  are also used for validation purposes) and reveals that the function  $X(L)$  is well  
430 approximated by regression line

431

$$X(L) = a_2 L + b_2, \quad (27)$$

432

433

434

435

436

437

$$\Delta D(\varepsilon, L) = \frac{\Delta n(\varepsilon, L)}{a_2 L} \quad (28)$$

438

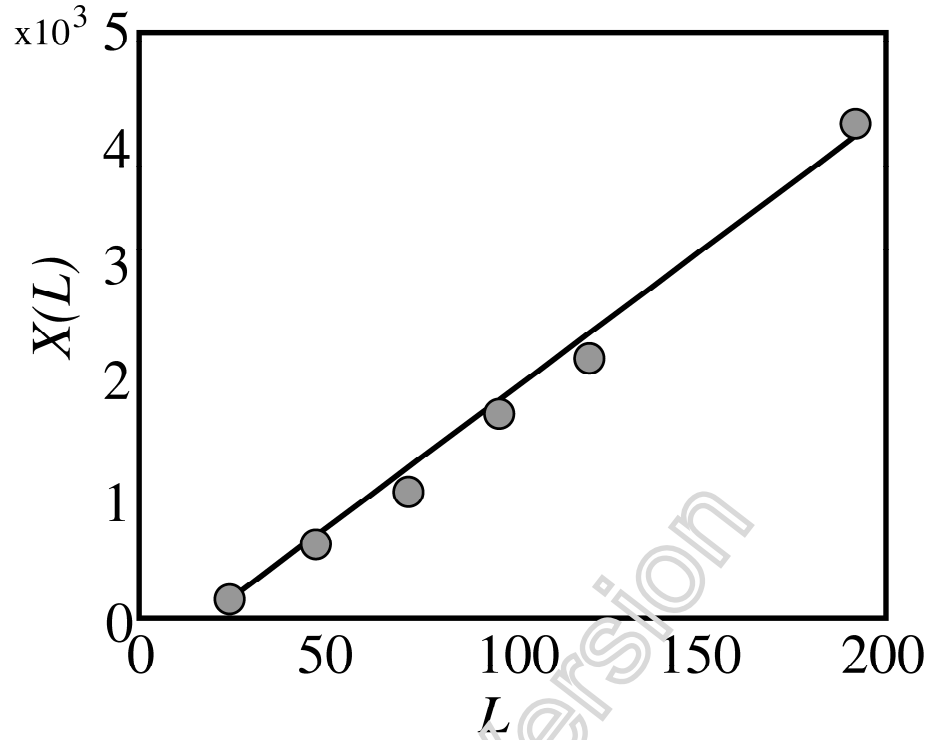
439

440

441

442

$$\Delta D(\varepsilon, L) = \frac{L^d a_1 \Delta \varepsilon + L^{d+\beta+\beta'} b_1 \left[ 1 - \exp\left(-c_1 \frac{\Delta \varepsilon}{L^{\beta+\beta'}}\right) \right]}{a_2 L} \quad (29)$$



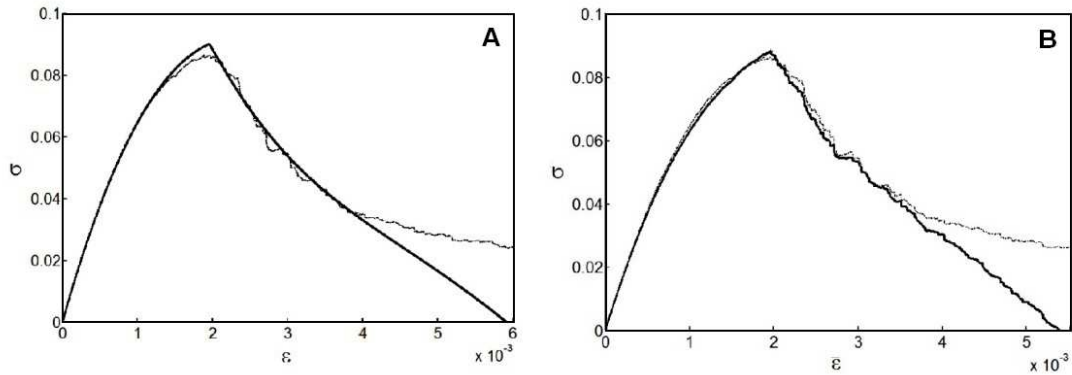
443

444 **Fig.11.** Comparison of  $X(L)$  estimated from Eq.(26) vs Eq. (27) from average data  $\Delta n$  (circles).

445

446 The application of Eq.(29) is shown in Fig.12a, where the model (4) now matches simulation  
 447 for most of the damage process. The scaling law (29) provides a convenient smooth analytical  
 448 relation for  $\Delta n(\varepsilon, L)$  but is clearly a trade-off between the need of having an average estimate of  
 449 the microcracks number valid for any lattice size and the inevitable loss of "details"  
 450 characterizing each individual curve, as made evident in Fig.12b when actual numerical data  
 451 for  $n$ ,  $N_p$ , and  $\Delta n$  are used directly in Eq.(28). Yet, the difference between the estimate of  $\Delta n$   
 452 from scaling (118) and the real value from simulations never exceeded 10% for any lattice size,  
 453 which confirms the robustness of the K-approach.

454



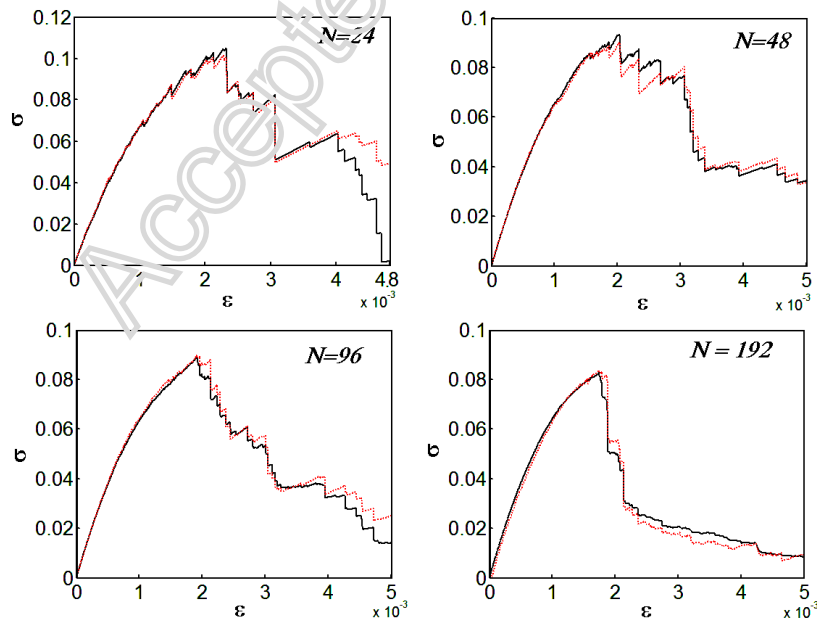
455

456 **Fig.12.** Complete model fit to average data for  $N=96$  from (A) analytical expression (29) vs.  
 457 and (A) scaling model (28), where actual numerical data for  $n$ ,  $N$ , and  $\Delta n$  are used directly.

458

459 Also the parameter  $X(L)$  contributes to the accuracy of the model. In fact, as shown by the four  
 460 randomly picked replicates of  $L = \{24, 48, 96, 192\}$  in Fig.13, the model (28) dramatically  
 461 improves and captures the damage response from individual simulations by using the exact  
 462 value for  $X(L)$  (“o” marks in Fig.11), thus further confirming the choice of damage parameter  
 463 and scaling laws.

464



465

466 **Fig. 13.** Responses of scaling model Eq.(17) and (28) from the “K-approach” (dotted line) vs.  
 467 original simulation data (solid line) for 4 random replicates for  $L = \{24, 48, 96, 192\}$  .

468

469

### 470 3.1.3. Summary of the procedure

471 In summary the “Krajcinovic approach” proposed herein consists of a two-steps scaling  
472 procedure encompassing the following:

473 1. Collection/simulation of  $\sigma$ - $\varepsilon$  and  $n$ - $\varepsilon$  for several samples and over a sufficiently large  $L$   
474 range (recommended 2 orders of magnitude) ;

475 2. Compute averages curves per each  $L$ ;

476 3. Subdivide the datasets in pre-peak and post-peak data;

477 4. Apply scaling Eq.(9) to the all data for the sake of scaling peak points into one;

478  $\rightarrow$ I check point: IF NOT POSSIBLE, THEN STOP

479 5. Compute approximate relations for  $n(\varepsilon;L)$ ,  $\varepsilon_p$  and  $D_p$  (the later one being scale-  
480 invariant);

481 6. Identify a suitable model/definition for the damage parameter in the fracture initiation  
482 regime;

483 7. Apply scaling Eq.(10) to the softening data seeking to transform the remaining of the  
484 data;

485  $\rightarrow$ II check point: IF NOT POSSIBLE, THEN STOP

486 8. Compute approximate relations for  $\Delta n(\varepsilon;L)$  and  $\Delta D_p$ ;

487 9. Identify a suitable model/definition for the damage parameter in the fracture  
488 propagation regime;

489 10. Validate the results of the scaling law and of the choice of D by comparing Eq.(4) vs.  
490 the initial datasets of simulations or experiments

## 491 4. CONCLUSIONS

492 For quite a few decades, lattice models have been focused on the investigation of finite-size  
493 scaling and on the formulation of physical/rational models of damage. They have appealed

494 specially to the community of physicists and mathematicians active in statistical physics who  
495 have seized the opportunity to investigate failure in heterogeneous systems by the same  
496 approaches developed for phase transitions and chaos. However, the K-approach developed  
497 here from lattice data is an heuristic scaling procedure bears the potential to evolve from  
498 science to a practical tool for the engineering community, being (i) based on the physics of the  
499 fracture initiation process underlying the damage in quasi-brittle-system and (ii) being  
500 transferable in principle also to experimental data, provided that the number of microcracking  
501 events is tracked along with the stress response. Approximate analytical expressions are readily  
502 deduced from scaled data and shown to yield robust stress vs. strain constitutive relations. Yet,  
503 this method has to be benchmarked against the current mainstream approached described in the  
504 introduction, contributing to the ongoing debate about size-effects modeling and control in  
505 quasi-brittle system.

506

507

508

509

## 510 **5. APPENDIX: LATTICE MODEL**

511 Fracture initiation in quasi-brittle materials has proved to be an elusive subject that has been  
512 approached by a continuum and discrete angle for over 20 years now. By a continuum  
513 standpoint, a substantial amount of work has been produced. The consideration of at least two  
514 length scales (see Fig. 14) poses an intrinsic difficulty for first displacement gradient  
515 continuum damage model (CDM), more suited to capture macroscopic effects (e.g. Chambolle  
516 et al, 2009, 2010; Contrafatto and Cuomo, 2002, 2005, 2006; Del Piero and Truskinovsky,  
517 2009; Rinaldi and Placidi 2013), and micropolar elasticity (e.g. Altenbach et al. 2010; Diebels  
518 and Geringer, 2013; Diebels and Scharding 2011; Eremeyev, 2005; Forest et al. 2001; Forest,  
519 2009) or higher displacement gradients (e.g. Diebels and Ebinger, 2005; Ebinger, Steeb,  
520 Diebels, 2005; Alibert, Seppecher and dell’Isola, 2003; Seppecher, Alibert, Dell’Isola, 2011)  
521 are required to capture damage localization (e.g. Sunyk and Steinmann, 2003; Yang and  
522 Misra, 2010).



523           Conversely, the problem can be approached from the bottom length scale using discrete  
524 microstructural models. These are a convenient and increasingly popular alternative pursued by  
525 many research groups besides those already cited (e.g. Curtin and Scher, 1990; Jagota and  
526 Bennison, 1995; Van Mier et al. 2002; Mastilovic, 2008, Rinaldi et al. 2008; Miguel et al.  
527 2010) for they are well suited for multiscale problems. They can incorporate several  
528 microstructural features into the model by using statistical information that can be measured  
529 directly and, without making extensive assumptions, are capable of scaling the material  
530 response to the macro level. In this class, considerable attention has been drawn by lattice  
531 models, which provide simple representations of complex systems, such as the disordered  
532 microstructures of ceramics, concrete and other quasi-brittle polycrystalline materials.  
533 Contrarily to a classical CDM, lattice models resolve individual grain boundaries and are  
534 convenient for study of brittle damage by intergranular cracking. Van Mier and coworkers  
535 (2002), for example, showed the agreement between simulated tensile tests and actual tests for  
536 concrete using lattice models of the microstructure. Some effort has been progressively  
537 devoted to bridge across discrete and continuum approaches, in the attempt to reconcile the  
538 two. For example, Rinaldi and Placidi (2013) established the connection between the present  
539 lattice models and 2<sup>nd</sup> gradient CDM by analyzing a case study that reveals such a consistency.  
540 The present paper is the complement to the latter work, addressing size effects and providing  
541 the continuum scaling laws discussed in the body text.

542           The details of the specific 2-D lattice model used in our discussion and presented in  
543 prior work (Rinaldi and Krajcinovic, 2007, Mastilovic and Krajcinovic, 1999) are briefly  
544 recalled here for convenience. The lattice is made of a disordered network of springs with finite  
545 strength, providing a first order approximation for the materials microtexture, the morphology  
546 of which can be represented by a random Voronoi froth and its dual Delaunay lattice. A  
547 Voronoi polygon represents a grain of ceramic, a concrete aggregate or a granule of clastic  
548 rock whereas a bond in the Delaunay lattices is representative of corresponding interface  
549 cohesion.

550           The lattice encapsulates both morphological and mechanical types of information at lower  
551 computational expense. Each grain of the polycrystalline material maps into a node in the  
552 lattice, while each lattice link marks a grain boundary and is a linear spring of stiffness  $k_{(ij)}$  and

553 finite tensile strength  $f_{ij}^{*+}$  (or positive elongation  $\Delta u_{ij}^{*+}$ ) that transmits the force between  
 554 adjacent i-th and j-th generic grains ( $i, j = 1..N_0$ , such that  $i \neq j$  and  $N_0 = \# \text{ nodes}$ )<sup>2</sup>

$$555 \quad f_{ij}(\mathbf{u}_i, \mathbf{u}_j; t, t_0) = \begin{cases} k_{ij}(\mathbf{u}_j - \mathbf{u}_i) \cdot \mathbf{r}_{ij} = k_{ij} \Delta u_{ij}(t) & (\Delta u_{ij}(t) < 0 \text{ or } 0 < \Delta u_{ij}(t_0) < \Delta u_{ij}^{*+}, \forall t_0 \in [0, t]) \\ 0 & (\Delta u_{ij}(t) > 0 \text{ and } \exists t_0 \in [0, t] \text{ such that } \Delta u_{ij}(t_0) = \Delta u_{ij}^{*+}) \end{cases} \quad (30)$$

556 (not a tensor)<sup>2</sup>

557 The springs behave as decohesive elements that break under tensile load when a “random  
 558 critical strain” is reached previously at any time point  $t_0$  between 0 and the current time  $t$ , thus  
 559 reproducing the intergranular cracking process of brittle materials such as concrete or ceramics.

560 For the data in this paper the following assumptions apply:

- 561 - the links have equal stiffness  $k_{ij} = k$  (=100) and equal length  $\ell_0$  (=1) breaking at a  
 562 tensile strain  $\varepsilon_{ij}^* = \Delta u_{ij}^{*+} / \ell_0$ ,
- 563 - no healing is allowed,
- 564 - the (mechanical) disorder is inserted in this lattice by sampling the failure tensile strains  
 565 from a uniform distribution  $p_f(\varepsilon)$  in the interval  $[0, 10^{-2}]$ .

566 Damage is introduced in the network by the rupturing of the links, which are removed  
 567 progressively from the system. Broken links remain active in compression if load reversal  
 568 occurs in the course of deformation to account for crack closure. The lattice is geometrically  
 569 distorted since the equilibrium link lengths are normally distributed within the range  
 570  $\alpha_l \bar{\lambda} \leq \lambda \leq (2 - \alpha_l) \bar{\lambda}$  with  $\alpha_l = 0.1$  (if  $\alpha_l = 1$  all grains are perfect hexagons).

571 Quasi-static displacement-controlled uniaxial tensile tests are simulated on different lattice  
 572 sizes  $L$  by means of a molecular dynamics solver based upon the Verlet's algorithm. Each  
 573 simulation is carried on incrementally up to the threshold of failure by applying small  
 574 displacement steps and by computing the equilibrium configuration at each step.

575 For the sake of the advocated similarity between the lattice and the fiber bundle model (FBM),  
 576 the latter one consists of an ensemble of parallel and non-interacting links of equal stiffness  $k$   
 577 connected by rigid bus bars at the ends, the damage parameter of which is  $D = \int p_f(\varepsilon) d\varepsilon$  (Rinaldi  
 578 2011). Under the conditions of uniform sampling distribution in our simulations, it is readily

<sup>2</sup> The index notation  $\varepsilon_{ij}$  refers to the ij-th link has end nodes i and j, not to be confused with second order tensors, as customarily reserved in solid mechanics.

579 obtained  $D = \varepsilon/0.01$ , according to which the stress response (4) is a parabola and  $Dp=0.5$ , as  
580 stated in Eq(16).

## 581 **References**

- 582 Alava MJ, Nukala PKVV, Zapperi S (2006) Statistical models of fracture. *Advances in*  
583 *Physics* 55 (3–4): 349–476
- 584 Alibert J.J., Seppecher P. , Dell’Isola F. (2003), Truss modular beams with deformation  
585 energy depending on higher displacement gradients, *Mathematics and Mechanics of*  
586 *Solids*, vol. 8, 51-73
- 587 Altenbach H, Eremeyev V.A., Lebedev L.P., Rendon L.A. (2010). Acceleration waves and  
588 ellipticity in thermoelastic micropolar media, *Arch. Appl. Mech.* 80. No 3. Pp. 217-227.
- 589 Balankin AS, Bravo-Ortega A, Galicia-Cortes MA, Susarey O (1996) The effect of self-affine  
590 roughness on crack mechanics in elastic solids. *Int J Fract* 79 (4): R63-R68
- 591 Barabasi AL, Stanley HE (1995) *Fractal Concepts in Surface Growth*. Cambridge University  
592 Press, Cambridge
- 593 Bazant ZP (1997), Scaling of quasibrittle fracture: asymptotic analysis. *Int J Fract* ;83(1):19–  
594 40.
- 595 Bazant ZP (1997), Scaling of quasibrittle fracture: hypotheses of invasive and lacunar  
596 fractality, their critique and Weibull connection. *Int J Fract*;83(1):41–65.
- 597 Bazant (2004), Scaling theory for quasibrittle structural failure, Zdenek P. Bazant), *PNAS*,  
598 vol 101, n 37, 13400–13407
- 599 Borodich FM (1997) Some fractal models of fracture. *J Mech Phys Solids* 45 (2): 239–259
- 600 Carpinteri A (1994) Fractal nature of material microstructure and size effects on apparent  
601 mechanical properties. *Mech Mater* 18: 89–101.
- 602 Carpinteri A, Corrado M, Lacidogna G (2012) Three different approaches for damage domain  
603 characterization in disordered materials: Fractal energy density, b-value statistics,  
604 renormalization group theory, *Mechanics of Materials* 53, 15–28A.
- 605 Chambolle A, Francfort G.A. and Marigo J.-J., (2010) Revisiting energy release rates in brittle  
606 fracture, *Journal of Nonlinear Science* 20, 395-424

607 Chambolle A, Francfort G.A. and Marigo J.-J., (2009) When and how do cracks propagate, J.  
608 Mech. Phys. Solids, 56 1614-1622

609 Chelidze TL (1982) Percolation and Fracture, Physics of the Earth. Planetary Interiors 28: 93

610 Cherepanov GP, Balankin AS, Ivanova VS (1995) Fractal fracture mechanics. Engng Fract  
611 Mech 51(6): 997-1033

612 Christensen K (2002) Percolation Theory (ebook). MIT, Cambridge

613 Contrafatto L, Cuomo M (2002), A new thermodynamically consistent continuum model for  
614 hardening plasticity coupled with damage, International Journal of Solids and Structures,  
615 39, 6241-6271

616 Contrafatto L, Cuomo M (2005), A globally convergent numerical algorithm for damaging  
617 elasto-plasticity based on the Multiplier method, Int. J. Numer. Meth. Engng, 63, 1089-  
618 1125

619 Contrafatto L, Cuomo M (2006), A framework of elastic-plastic damaging model for concrete  
620 under multiaxial stress states, International Journal of Plasticity, 22, 2272-2300

621 Curtin W.A., Scher H. (1990) Brittle fracture in disordered materials, J. Mater. Res., Vol 5, 3,  
622 535-553

623 D'Annibale F., Luongo A. (2012) A damage constitutive model for sliding friction coupled to  
624 wear. Continuum Mechanics and Thermodynamics, doi: 10.1007/s00161-012-0283-4

625 De Arcangelis L, Redner, S, Herrmann HJ (1985) A random fuse model for breaking  
626 processes. J Phys Lett 46: 585-590

627 Del Piero G, Truskinovsky L (2009) Elastic bars with cohesive energy, Continuum Mech.  
628 Thermodyn. 21, 141-171

629 Diebels S., Ebinger T., Steeb H. (2005), An anisotropic damage model of foams on the basis  
630 of a micromechanical description, J. Mat. Sci., 40, 5919-5924.

631 Diebels S, Scharding D (2011), From lattice models to extended continua, In B. Markert  
632 (Hrsg.), Advances in Extended and Multifield Theories for Continua, Lecture Notes in  
633 Applied and Computational Mechanics, Springer, pp. 19-45.

634 Diebels S, Geringer A, (2013) Micromechanical and macromechanical modelling of foams:  
635 Identification of Cosserat parameters, ZAMM, published online, DOI  
636 10.1002/zamm.201200271.

637 Duxbury PM, Beale PD, Leath PL (1986) Size Effects of Electrical Breakdown in Quenched  
638 Random Media. *Phys Rev Lett* 57 (8): 1052-1055

639 Ebinger T, Steeb H, Diebels S (2005), Anisotropic damage for higher order continuum  
640 models, *Proc. Appl. Math. Mech.*, 5, 331-332.

641 Eremeyev V.A.(2005), Acceleration waves in micropolar elastic media, *Doklady Physics*, 50.  
642 No. 4. Pp. 204–206

643 Family F, Vicsek T (1991) *Dynamics of fractal surfaces*. World Scientific, Singapore

644 Feng S, Thorpe MF, Garboczi E (1985) Effective-medium theory of percolation on central-  
645 force elastic networks. *Phys Rev B* 31 (1): 276-280

646 Forest S, Pradel F. and Sab K. (2001), Asymptotic analysis of heterogeneous Cosserat media,  
647 *Int. J. Solids Struct.* 38, 4585-4608

648 Forest S, (2009) Micromorphic approach for gradient elasticity, viscoplasticity and damage, *J.*  
649 *Eng. Mech.* 135, 117-131

650 Garcia-Molina R, Guinea F, Louis E (1988) Percolation in isotropic elastic media. *Phys Rev*  
651 *Lett* 60: 124-127

652 Guyon E, Roux S, Hansen A, Bideau D, Troadec JP, Crapon H (1990) Non-local and non-  
653 linear problems in the mechanics of disordered systems: application to granular media and  
654 rigidity problems. *Rep Prog Phys* 53, 373-419

655 Hansen A, Roux S, Herrmann HJ (1989) Rupture of central-force lattices. *J Phys France* 50:  
656 733-744

657 Hansen A, Roux S (2000) *Statistics Toolbox for Damage and Fracture*. In: Krajcinovic D, Van  
658 Mier JGM (eds): *Damage and Fracture of Disordered Materials*. Springer, Berlin  
659 Heidelberg New York

660 Herrmann HJ, Hansen A, Roux S (1989) Fracture of disordered, elastic lattices in two  
661 dimensions. *Phys Rev B* 39 (1): 637–648

662 Ince R, Arslan A, Karihaloo BL (2003) Lattice modeling of size effect in concrete strength.  
663 *Eng Fract Mech* 70(16): 2307–2320

664 Jagota A., Bennison S.J. (1995) Element Breaking Rules in Computational Models for Brittle  
665 Fracture, *Modelling and Simulation in Materials Science and Engineering*, Vol 3, pp 485-  
666 501

667 Kachanov L.M. (1958) On creep rupture time, *Izv. Akad. Nauk.* 8, 26–31

668 Krajinovic, (1996) *Damage Mechanics*. North-Holland, Amsterdam, The Netherlands  
669 Krajinovic D, Rinaldi A (2005a) *Thermodynamics and Statistical Physics of Damage*  
670 *Processes in Quasi-Ductile Solids*. *Mech Mater* 37: 299-315  
671 Krajinovic D, Rinaldi A (2005b) *Statistical Damage Mechanics - 1. Theory*. *J Appl Mech* 72:  
672 76-85  
673 Mastilovic S, Krajinovic K (1999a) *High-velocity expansion of a cavity within a brittle*  
674 *material*. *J Mech Phys Solids* 47: 577-610  
675 Mastilovic S, Krajinovic D (1999b) *Penetration of Rigid Projectiles Through Quasi-Brittle*  
676 *material*. *J Appl Mech* 66: 585-592  
677 Mastilovic S (2008) *A Note on Short-Time Response of Two-Dimensional Lattices During*  
678 *Dynamic Loading*, *International Journal of Damage Mechanics* 17, pp. 357-361  
679 Miguel L.F.F., Iturrioz I. , Riera J. D. (2010), *Size Effects and Mesh Independence in*  
680 *Dynamic Fracture Analysis of Brittle Materials*, *Computer Modeling in Engineering &*  
681 *Sciences*, 56, pp. 1-16  
682 Mishnaevsky Jr LL (1996) *Determination for the time-to-fracture of solids*. *Int J Fract* 79 (4):  
683 341-350  
684 Nukala PKVV, Simunovic S, Mills RT (2006) *Statistical physics of fracture: scientific*  
685 *discovery through high-performance computing*. *J Phys* 46: 278-291  
686 Ostoja-Starzewski M (1989) *Damage in Random Microstructure: Size Effects, Fractals and*  
687 *Entropy Maximization*. In: *Mechanics Pan-America 1989*, C.R. Steele et al. (eds.), ASME  
688 Press, pp 202-213  
689 Ostoja-Starzewski M. (2007) *Microstructural randomness and scaling in mechanics of*  
690 *materials*. Taylor & Francis Group, Boca Raton  
691 Ostoja-Starzewski M, Li J, Joumaa H, Demmie PN (2013) *From fractal media to continuum*  
692 *mechanics*. *Zeit Angew Math Mech (ZAMM)* 93: 1-29  
693 Pugno NM, Ruoff RS (2004) *Quantized fracture mechanics*. *Phil Mag* 84: 2829  
694 Rinaldi A, Mastilovic S, Krajinovic D (2006) *Statistical Damage Mechanics - 2. Constitutive*  
695 *Relations*. *J Theor Appl Mech* 44 (3): 585-602  
696 Rinaldi A, Krajinovic D., Peralta P., Lai Y.-C., (2008) *Modeling Polycrystalline*  
697 *Microstructures With Lattice Models: A Quantitative Approach*, *Mech. Mater.*, 40, 17-36

698 Rinaldi A, Krajcinovic D, Mastilovic S (2007) Statistical Damage Mechanics and Extreme  
699 Value Theory. *Int J Damage Mech* 16(1): 57-76

700 Rinaldi A. and Lai Y.-C. (2007), Statistical damage theory of 2d lattices: energetics and  
701 physical foundations of damage parameter, *Int. J. Plasticity*, Vol 23, pp 1796–1825

702 Rinaldi A (2009) A Rational Model for 2D Disordered Lattices Under Uniaxial Loading. *Int J*  
703 *Damage Mech* 18: 233-257

704 Rinaldi A (2011), Statistical model with two order parameters for ductile and  
705 soft fiber bundles in nanoscience and biomaterials, *Phys Rev E (Stat Nonlin Soft Matter*  
706 *Phys)*, 83(4-2): 046126

707 Rinaldi A, Placidi L (2013) A microscale second gradient approximation of the damage  
708 parameter of quasi-brittle heterogeneous lattices, DOI: 10.1002/zamm.201300028

709 Roux S, Guyon E (1985) Mechanical percolation: a small beam lattice study. *J Phys Lett* 46:  
710 L999–L1004

711 Sen PN, Feng S, Halperin BI, Thorpe MF (1985) Elastic Properties of Depleted Networks and  
712 Continua. In: Boccara N, Daoud M (eds) *Physics of Finely Divided Matter*. Springer,  
713 Berlin Heidelberg New York, pp 171-179

714 Seppecher P., Alibert J.J., and Dell’Isola F. (2011), Linear elastic trusses leading to continua  
715 with exotic mechanical interactions, *Journal of Physics: Conference Series*, vol. 319, no. 1,  
716 p. 012018. IOP Publishing.

717 Sunyk R., Steinmann P. (2003). On Higher Gradients in Continuum-Atomistic Modelling, *Int.*  
718 *J. Solids Structures* 40, Nr. 24, S. 6877-6896

719 Stauffer D, Aharony A (1994) *Introduction to Percolation Theory*. Taylor & Francis, London

720 Tarasov VE (2013) Review of Some Promising Fractional Physical Models. *Int J Modern*  
721 *Phys* 27(9): 1330005

722 Sunyk R, Steinmann P (2003), On Higher Gradients in Continuum-Atomistic Modelling, *Int.*  
723 *J. Solids Structures* 40, Nr. 24, S. 6877-6896

724 Yang Y, Misra A (2010), Higher-Order Stress Strain Theory for Damage Modeling  
725 Implemented in an Element-free Galerkin Formulation, *CMES* 1549(1), 1-36

726 Van Mier J.G.M., Vliet M.R.A., Wang T.K. (2002), Fracture mechanisms in particle  
727 composites: statistical aspects in lattice type analysis. *Mech. Mater.* , 34, 705–724

728 Wnuk M, Yavari A (2008) Discrete fractal fracture mechanics. Engng Fract Mech 75: 1127–  
729 1142

Accepted Version